MICHIGAN STATE UNIVERSITY

CYCLOTRON LABORATORY

NEUTRON INCLUSIVE MEASUREMENTS OF ^{36}Ar + Ag REACTIONS AT 35 MeV/NUCLEON

D. SACKETT, A. GALONSKY, C.K. GELBKE, H. HAMA,
L. HEILBRONN, D. KROFCHECK, W. LYNCH,
H.R. SCHELIN, M.B. TSANG, X. YANG, F. DEAK,
A. HORVATH, A. KISS, Z. SERES, J. KASAGI,
and T. MURAKAMI

DECEMBER 1990

MSUCL-754

MSUCL-754
December, 1990

Neutron inclusive measurements of $^{36}Ar+Ag$ reactions at 35 MeV/nucleon

D. Sackett, A. Galonsky, C.K. Gelbke, H. Hama[§], L. Heilbronn, D. Krofcheck[†], W. Lynch, H.R. Schelin[‡], M.B. Tsang, and X. Yang*.
National Superconducting *Cyclotron* Laboratory, *and* Department *of Physics* and Astronomy, Michigan State University, *East Lansing,* Michigan 48824

F. Deák, A. Horváth, and A. Kiss
Department of Atomic Physics, Eötvös University, *Budapest 114, Hungary H-1088*

Z. Seres
Hungarian *Academy* of Sciences, Central *Research Institue for Physics,* Budapest *114, Hungary H-15.25*

J. Kasagi
Department *of Physics, Tokyo Institute of* Technology, 0-Okayama, Meguro-Ku, *Tokyo,* Japan.

T. Murakami
Department *of Physics, Kyoto University, Kitasherakawa, Kyoto* 606, Japan

Abstract

We have measured the inclusive neutron cross section as a function of neutron energy and angle at 15 °, 30 °, 45 °, 60 °, 120 °, and 160 ° for the system $Ag(^{36}Ar,n)$ at 35 MeV per nucleon. All spectra can be fitted with a standard moving source model consisting of a projectile-like source, an intermediate rapidity source, and a target-like *source.* Temperatures for the target-like and intermediate rapidity source were found to be about 4 MeV and 11 MeV, respectively. Neutron multiplicities for each were 5.6 and 1.0. These parameters are compared with those from the neutron inclusive measurement of $Ag(^{14}N,n)$ at 35 MeV per nucleon and with proton exclusive data from the reaction $^{32}S+Ag$ at 30 MeV/nucleon.

1. INTRODUCTION

A good deal can be learned about heavy ion reactions by examining the resulting neutron spectra. Typically, neutron yields are considered in coincidence with fragments,[1-5] but many of the gross features of the reaction mechanism, and properties such as multiplicities and nuclear temperatures, can be deduced from inclusive experiments as well.[6,7] It is our goal to measure changes in the pattern of neutron emission to try to understand the nature of heavy ion reactions. Although impact parameter selection is unavailable in an inclusive experiment, it will be shown that contributions from distinct sources can be unfolded from the neutron spectra using

a standard moving source model. Although the model relies only on classical thermodynamics, it is encouraging that the values of the fitted parameters have some systematic agreement over a wide range of reacting systems. We also compare the resulting thermal fit parameters with those from the reaction Ag(^{14}N,n) at 35 MeV per nucleon and with proton exclusive spectra from a ^{32}S + Ag at 30 MeV per nucleon.

2. EXPERIMENTAL PROCEDURE

Using a 35 MeV per nucleon $^{36}Ar^{11+}$ beam provided by the K500 Cyclotron at Michigan State University, we have measured inclusive neutron spectra from the reaction Ag(^{36}Ar,n) at angles of 15°, 30°, 45°, 60°, 120° and 160°. The target consisted of 2.57 mg/cm^2 of natural silver, rotated 30° clockwise with respect to the beam direction. Energy loss of the projectile through half the rotated target only amounted to 0.1 MeV/nucleon. The detectors and the measurement technique are described in detail in ref. 7. Figure 1 shows the experimental set-up. Detectors on the left side of the beam (positive angles) were positioned with flight paths ranging from 160 to 250 cm. These detectors provided the low energy neutron spectrum. To achieve better energy resolution when detecting higher energy neutrons, detectors on the right side of the beam (negative angles) were placed at distances ranging from 350 to 450 cm. For these flight paths, several detectors were bundled together to provide a counting rate similar to that of the detectors at positive angles. The hatched rectangular regions represent cylindrical brass or steel bars (shadow bars) ranging from 20 to 30 cm in length. Data collected without the bars includes neutrons from the target and inscattering from other areas of the vault or chamber. Data collected with the bars shadowing the detector from the target comprises all the background neutrons. Subtracting these spectra then gives only the neutron yields from the target. The small lines in front of the detectors or shadow bars represent veto paddles. They are thin plastic scintillators that are used to reject high energy protons and deuterons that enter the neutron detectors. All charged particles with $Z \geq 2$ are stopped in the material between the target and detectors.

The timing was performed as follows: an event in a detector served as a start signal for a time-to-digital converter (TDC). The cyclotron period was $\sim$ 52 ns, so a TDC stop signal from the cyclotron RF, scaled by a factor of two, came $\sim$ every 104 ns. Half of a typical time-of-flight spectrum is shown in Figure 2 (the other half would be a similar spectrum betweem channels 175 and 275). Shown are both the total neutron spectrum (including background) and the background contribution. Also shown is the location of the gamma ray peak. From the location of the gamma ray in the time-of-flight spectrum and a calibration (ns/channel) of the time-to-digital converter, the neutron time-of-flight can be calculated directly. Neutrons were distinguished from gamma rays using pulse shape discrimination.[8] Neutron detector efficiencies, typically between 10 and 20%, were calculated from a Monte Carlo code KSUVAX.[8] The uncertainty in the efficiencies is 10%.[9]

The neutron yields are binned as counts per time bin versus time-of-flight. Converting the time-of-flight bin to an energy bin gives the neutron yield in counts per MeV versus energy. The neutron yields are attenuated when passing through the steel scattering chamber and, for some angles, up to ten millimeters of silicon (due

to the fragment telescopes). Where no silicon is present typical attenuations are 13% for 25 MeV neutrons and 8% for 75 Mev neutrons. When the flight path contained the silicon telescopes, attenuations for 25 Mev neutrons were about 25%, and for 75 MeV neutrons about 18%. Folding in the detector efficiency and the percentage of attenuation gives the final neutron energy spectrum.

Because the cyclotron period is only 52 ns, the low energy spectrum is contaminated by high energy neutrons from a subsequent beam pulse. To obtain the low energy neutron spectrum, the high energy contribution was subtracted using the following technique: Setting a high pulse height threshold for the detector provides the high energy spectrum with no overlapping low energy contribution. At a low threshold, this spectrum changes only by the ratio of detection efficiencies for the high and low thresholds, hence the high energy neutron spectrum at low pulse height thresholds can be obtained. This scaled high energy spectrum is then subtracted from a neutron spectrum obtained at a low threshold, thus leaving an uncontaminated low energy spectrum. For detectors at positive angles, low energy thresholds of 4.0-6.0 MeV (neutron energy) were used.

3. RESULTS AND DISCUSSION

Figure 3 shows the double differential neutron cross section data. It is the behavior of the energy spectra that justifies a moving source analysis. At 45 ° and 60 ° the spectra appear to be superpositions of two distinct components which vary exponentially with energy. In terms of a nuclear temperature, the low energy neutron data possess a steeper slope, therefore indicating a cooler source. The higher energy neutrons stem from a hotter source, because the slope of the data is much flatter. The spectra at 120 ° and 160 ° decrease exponentially with increasing energy. Because the data at 120 ° and 160 ° have such similiar magnitudes, it can be inferred that the source is moving slowly enough to provide nearly isotropic emission. The enhancement in the 15 ° spectrum arises from rapidly moving sources created by peripheral collisions, so their contribution appears only at forward angles. To proceed with the fitting, it is assumed that the sources are Maxwellian in nature and emit neutrons isotropically in their own rest frames. Assuming volume emission, the neutron distribution in a source rest frame is:

$$\frac{d^2\sigma_n}{dE'd\Omega'} = \frac{N\sqrt{E'/\pi}}{2\pi T^{3/2}} \exp\left[\frac{-E'}{T}\right]$$

Here E' is the neutron energy in the source rest frame, Ω' is the solid angle in the source rest frame, T is the temperature in MeV and N is the neutron production cross section in barns. E' is related to the lab neutron energy E by:

$$E' = E + \epsilon - 2\sqrt{\epsilon E}\cos\theta$$

where ϵ is the kinetic energy per nucleon of the source and θ is the laboratory scattering angle. Summing over three sources, the parameterization in the laboratory frame of reference takes the form:

$$\frac{d^2\sigma_n}{dEd\Omega} = \sum_{i=1}^{3} \frac{N_i\sqrt{E/\pi}}{2\pi T_i^{3/2}} \exp\left[-\left[\frac{E - 2\sqrt{\epsilon_i E}\cos\theta + \epsilon_i}{T_i}\right]\right]$$

The nine fit parameters are N, T and ϵ for each source. The fitting was performed using a χ^2 minimization procedure. The χ^2 per degree of freedom was 3.71. Uncertainties correspond to the change in a parameter that increases χ^2 by 1, with all other parameters fixed at their optimum values.[11]

Table 1 summarizes the best fit values of the parameters, and Figure 3 displays the data and the overall fit. The values of the fit parameters confirm the characterisitics attributed to each source. Thus, the moving source analysis, while providing a good fit to the data, also contains a reasonable description of the reaction dynamics. For example, there is a slowly moving target-like source (TLS) that de-excites via neutron and charged particle evaporation, and a hotter (T$\approx$11 MeV) intermediate rapidity source (IRS) moving with V$\approx$V$_{beam}$/2 that de-excites in a similar manner. Finally, there is a projectile-like source (PLS) moving with a speed close to the beam velocity. Because the PLS originates from peripheral collisions, it must be noted that the assumption of thermal equilibrium, although convenient, is an oversimplification.[12] This source is included in the parameterization because it provides a useful fit to the spectra at the most forward angles. The remaining parameter, the neutron cross section N$_i$, is related to the multiplicity of the ith source as $M_i = N_i/\sigma_{tot}$. The total reaction cross section is calculated from:

$$\sigma_{tot} = \pi[r_0(36^{1/3} + 108^{1/3})]^2 = 3.40 \text{ b. with } r_0 = 1.29 \text{ fm.}^7$$

A 10% error is assumed in σ_{tot}.[7] The calculated neutron multiplicities are also shown in Table 1. The multiplicities are also meaningful in terms of the moving source analysis. The low energy part of the spectrum is well described by a purely exponential function of energy, and is attributed to a target-like remnant that de-excites via neutron and charged particle evaporation. Coincidence measurements of neutrons and intermediate mass fragments ($3 \leq Z \leq 5$)[5] or neutrons and heavy residues[13] for systems with similar targets and beam energies find TLS multiplicites between 5-7, in agreement with our result of 5.6. The intermediate-rapidity source models the early stage of the reaction, where nucleon-nucleon collisions largely determine the spectrum. For beam energies around 30-35 MeV/nucleon, neutron multiplicities ranging from one to three have been found[5,14], again in agreement with our value of 1.1.

4. COMPARISON WITH OTHER EXPERIMENTS

The most direct comparison can be made with the data of Schelin *et al.*[7] They have measured inclusive neutron spectra for ^{14}N on Ag at 35 MeV per nucleon. Table 1 compares their moving source parameters (in parenthesis) to ours. The final column in Table 1 represents the kinetic energy of the neutrons from the ith source, evaluated in the center of mass system. This kinetic energy is calculated from:

$$E'_{n_i} = \int_0^\infty \frac{dN_i(E')}{dE'} E' dE'$$

$\frac{dN_i}{dE'}$, the number of neutrons/MeV from the ith source, is:

$$\frac{dN_i}{dE'} = \frac{1}{\sigma_{tot}} \left(\frac{d\sigma_n}{dE'} \right)_i$$

where σ_{tot} is the total reaction cross section defined previously. Explicitly, the integral appears as:

$$E'_{n_i} = \frac{2N_i}{\sqrt{\pi}\sigma_{tot} T_i^{3/2}} \int_0^\infty E'^{3/2} e^{-E'/T_i} dE' = \frac{3}{2} M_i T_i$$

a. Target-like source

For the target-like source, the multiplicities and temperatures are approximately the same for both systems. Since the temperature of the source is directly related to it's excitation energy, this is a surprising result when the available energy in the center of mass reference frame (E'_{cm}) is considered. For the nitrogen projectile, E'_{cm} is 434 MeV, and for the argon beam E'_{cm} is 945 MeV, an increase by a factor of 2.2. It would seem that a large increase in excitation energy would create a more highly excited TLS, thus causing signifcant changes in the temperature and multiplicity parameters. The data implies that this is not happening. The source multiplicities and temperatures (and therefore excitation energies) are essentially the same for each projectile. Also, the total kinetic energy of the emitted neutrons (final column of Table 1) only changes from 27 MeV (nitrogen beam) to 35 MeV for the argon beam, an increase of about 30%. One possible explanation is that, for either projectile, the TLS evaporates it's lightly bound neutrons, but as it becomes more neutron deficient, separation energies increase such as to suppress further emission. Another factor is that with a larger projectile (argon) the geometric probability of incomplete fusion versus complete fusion is greater. By incomplete fusion, we mean any collision where a significant projectile-like spectator is formed. Of course, at higher excitation energies, new fragmentation decay channels may become available such that neutron evaporation is de-emphasized. In fact, fragment multiplicities (M_{frag}) for both projectiles on a silver target have recently been measured.[15] For the nitrogen projectile, M_{frag}=0.06 while for the argon beam, M_{frag}=0.33, an increase by a factor of 5.5.

It is also interesting to compare proton spectra from a similar reaction. Wada *et al.*[10] have determined temperatures, multiplicites and source velocities in a similar three source model for light charged particles ($Z \leq 2$) in coincidence with heavy residues and fragments for a 30 MeV/nucleon ^{32}S beam on a silver target. Individual sets of parameters are given for reactions based on 40%, 60%, 80% and 100% of full momentum transfer between projectile and target. This is essentially an indication of the impact parameter of the reaction, since a large percentage of projectile momentum transferred to the target implies a more central collision. Because an inclusive experiment measures yields without regard to the centrality of the collision, it seems appropriate to average the parameters for the proton data over the percentages of full momentum transfer before comparing to our neutron inclusive results. The results appear in brackets in Table 1. The source velocities in the data of Wada *et al.* are given as ratio of source velocity to beam velocity (β_s/β_{inc}). These can be transformed to the source kinetic energy per nucleon (ϵ_i). The compound nucleus source in their work is equated to our target-like source. The multiplicities for the TLS are lower,

but this can be attributed to the coulomb barrier that restricts low energy proton emission. The remaining parameters are in reasonable agreement.

b. Intermediate-rapidity source

The IRS describes the contribution to the neutron spectra from the early part of the interaction between projectile and target, where individual nucleon-nucleon collisions are important. In this regime, the velocity of the projectile nucleons is a major factor in determining the resulting neutron kinetic energy spectra. For the experiments with argon and nitrogen projectiles, the nucleon velocities are identical, so similar kinetic energy spectra are expected. Because the source temperature reflects the resulting kinetic energy spectra, the temperatures should therefore be similar. From Table 1, this is certainly the case. For argon and nitrogen projectiles the IRS temperatures are 11.4 and 11.1 MeV respectively. Because the argon projectile is more massive and therefore contributes more kinetic energy to the target, the energy will be dissipated over a larger region of the target. Thus the source size is expected to increase, but not the temperature. It is also interesting that the IRS temperature for the proton exclusive data of Wada *et al.* (T=11.0 MeV), is in agreement with the neutron inclusive source temperatures.

Again referring to Table 1, we find that there is only a small increase in the IRS multiplicity (from 0.86 to 1.1) for the Ag(^{36}Ar,n) reaction, compared to the Ag(^{14}Ar,n) reaction. This is a surprising result, considering that IRS neutron spectra are largely determined by nucleon-nucleon collisions, and that there are $\sim$ 2.6 times as many nucleons in the argon projectile. Possibly the same effects that suppress the TLS multiplicity exist here also. Refering to the data of Hama *et al.*[15], the fragment multiplicities for the nitrogen and argon beams are 0.08 and 0.38 respectively, an increase by about a factor of 5. The IRS proton multiplicity of Wada is similar to the neutron multiplicity with the argon projectile. Unlike the TLS, which describes predominantly low energy spectra, the IRS is responsible for the high energy part of the spectra, so coulomb barrier effects are no longer significant.

c. Projectile-like source

Since the main difference between the Ar+Ag and N+Ag systems is the size of the projectile, it should not be surprising that the fit parameters for the PLS are affected the most. The multiplicity for the argon projectile is $\sim$ 3 times greater, which should be expected since there are $\sim$ 2.6 times as many neutrons in the argon projectile. Also, the temperature and the total neutron kinetic energy (E'_n) are higher, whereas the source velocity is a bit lower. This implies a greater exchange of energy and momentum between target and projectile for grazing collisions. The PLS parameters of Wada *et al.* are also listed in Table 1. The values for temperature and kinetic energy per nucleon are in agreement with the Ar+Ag fit parameters, although the multiplicity is significantly different. Again, coulomb barrier effects may be affecting proton emission. However, it must be re-emphasized that treating the PLS as a thermal source is an oversimplification[12], hence comparison of thermal fit parameters should not be taken too literally.

5. CONCLUSIONS

We have measured the inclusive neutron spectra for the reaction Ag(^{36}Ar,n) at 35 MeV/nucleon. The energy spectrum at several angles can be fitted with three moving sources, and the resulting fit parameters are physically reasonable. Comparing our temperatures, multiplicites and total neutron kinetic energies to values found in previous lower energy work, we find that a large increase in available excitation energy does not manifest itself in more highly excited sources and higher neutron multiplicities. One explanation is that there may be alternative modes of de-excitation at higher energies. Further studies measuring both inclusive and exclusive neutron spectra over ranges of bombarding energies, with the same target and projectile, would provide the systematics to study this interesting effect.

6. ACKNOWLEDGEMENTS

Support of the U.S. National Science Foundation under Grants No. Int-86-17683 and No. Phy-86-11210 and of the Hungarian Academy of Sciences is gratefully acknowledged.

§ UVSOR, Institute for Molecular Science, Myodaiji, Okazaki 444, Japan.

† Current address: Lawrence Livermore National Laboratory, Livermore CA.

‡ Permanent address: Centro Tecnico Aeroespacial and supported in part by CNPq, Brazil.

* Current address: Ohio University, Athens, Ohio 45701

[1] D. Hilscher, J.R. Birkelund, A.D. Hoover, W.U. Schröder, W. W. Wilcke, J.R. Huizenga, A.C. Mignerey, K.L. Wolf, H.F. Breuer, and V.E. Viola, Phys. Rev C **20**, 576 (1979).

[2] Y. Eyal, A. Gavron, I. Tserruya, Z. Fraenkel, Y. Eisen, S. Wald, R. Bass, G.R. Gould, G. Kreyling, R. Renfordt, K. Stelzer, R. Zitzmann, A. Gobbi, U. Lynen, H. Stelzer, I. Rode, and R. Bock, Phys. Rev. Lett. **41**, 625 (1978).

[3] A. Galonsky, G. Caskey, L. Heilbronn, B. Remington, H. Schelin, F. Deak, A. Kiss, Z. Seres, and J. Kasagi, Phys. Lett. B **197**, 511 (1987).

[4] F. Deak, A. Kiss, Z. Seres, G. Caskey, A. Galonsky, C. K. Gelbke, B. Remington, M.B. Tsang, and J.J. Kolata, Nucl. Phys. **A464**, 133 (1987).

[5] C. Bloch, W. Benenson, A. Galonsky, E. Kashy, J. Heltsley, L. Heilbronn, M. Lowe, R.J. Radtke, B.R. Remington, J. Kasagi, and D.J. Morrissey, Phys. Rev. C **37**, 2469, (1988).

[6] D. Fox, D.A. Cebra, J. Karn, C. Parks, G.D. Westfall, and W.K. Wilson, Phys. Rev. C. **36**, 640 (1987).

[7] H.R. Schelin, A. Galonsky, C.K. Gelbke, L. Heilbronn, W.G. Lynch, T. Murakami, M.B. Tsang, X. Yang, G. Zhang, B.A. Remington, F. Deak, A. Kiss, Z. Seres, and J. Kasagi, Phys. Rev. C **39**, 1827 (1989).

[8] J. Heltsley, L. Brandon, A. Galonsky, L. Heilbronn, B.A. Remington, S. Langer, A. VanderMolen, and J. Yurkon, Nucl. Instrum. Methods Phys Res. A **263**, 441 (1988).

[9] R.A. Cecil, B.D. Anderson, and R. Madey, Nucl. Instrum. Methods **161**, 439 (1979).

[10] R. Wada, D. Fabris, K. Hagel, G. Nebbia, Y. Lou, M. Gonin, J.B. Natowitz, R. Billerey, B. Cheynis, A. Demeyer, D. Drain, D. Guinet, C. Pastor, L. Vagneron, K. Zaid, J. Alarja, A. Giorni, D. Heuer, C. Morand, B. Viano, C. Mazur, C. Ngô, S. Leray, R. Lucas, M. Ribrag, and E. Tomasi, Phys. Rev. C **39**, 497 (1989).

[11] P.R. Bevington, Program in CURFIT in *Data Reduction and Error Analysis for the Physical Sciences* (McGraw-Hill, New York, 1969), p. 237.

[12] A. Kiss, F. Deak, Z. Seres, G. Caskey, A. Galonsky, L. Heilbronn, B.A. Remington, and J. Kasagi, Phys. Lett. B **184**, 149 (1987).

[13] J. Galin, Proceedings of the Third International Conference on Nucleus-Nucleus Collisions, Saint-Malo, France, 1988.

[14] D. Hilscher, H. Rossner, A. Gamp, U. Jahnke, B. Cheynis, B. Chambon, D. Drain, C. Pastor, A. Giorni, C. Morand, A. Dauchy, P. Stassi, and G. Petitt, Phys. Rev. C **36**, 208 (1987).

[15] H. Hama *et al.* to be published.

Source	T (MeV)	ϵ (MeV/nucleon)	N (barns)	Multiplicity	E'_n (MeV)
TLS	4.2 ± 0.3	0.56 ± 0.13	19.1 ± 1.7	5.6 ± 0.7	35 ± 7
	(4.0 ± 0.2)	(0.45 ± 0.02)	(12.2 ± 1.1)	(4.5 ±0.6)	(27 ± 6)
	[5.4 ± 0.4]	[0.83]		[2.4 ±0.2]	
IRS	11.4 ± 1.3	11.77 ± 2.0	3.9 ± 0.5	1.1 ± 0.2	20 ± 6
	(11.1 ± 0.6)	(12.8 ±0.5)	(2.32 ± 0.2)	(0.86 ± 0.11)	(14 ± 3)
	[11.0 ± 1.2]	[14.3 ± 1.9]		[1.5 ± 0.2]	
PLS	3.6 ± 0.4	24.6 ± 1.8	3.2 ± 0.4	0.9 ± 0.1	5 ± 1
	(2.2 ± 0.3)	(30.1 ± 3.6)	(0.71 ± 0.06)	(0.26 ± 0.04)	(1 ±0.3)
	[4.0 ± 0.7]	[28.0]		[0.15 ± 0.06]	
Totals				7.6 ± 0.7	60 ± 9
				(5.6 ± 0.7)	(42 ± 7)

Table 1. Temperatures, source velocities, source strengths and multiplicities for a three source fit to the neutron spectra for the reaction ^{36}Ar(Ag,n). The data of Schelin *et al.* is in paranthesis and that of Wada *et al.* is in brackets. Missing uncertainties denote a fixed parameter in the fitting procedure. The final column is the total kinetic energy of the neutrons from the i^{th} source.

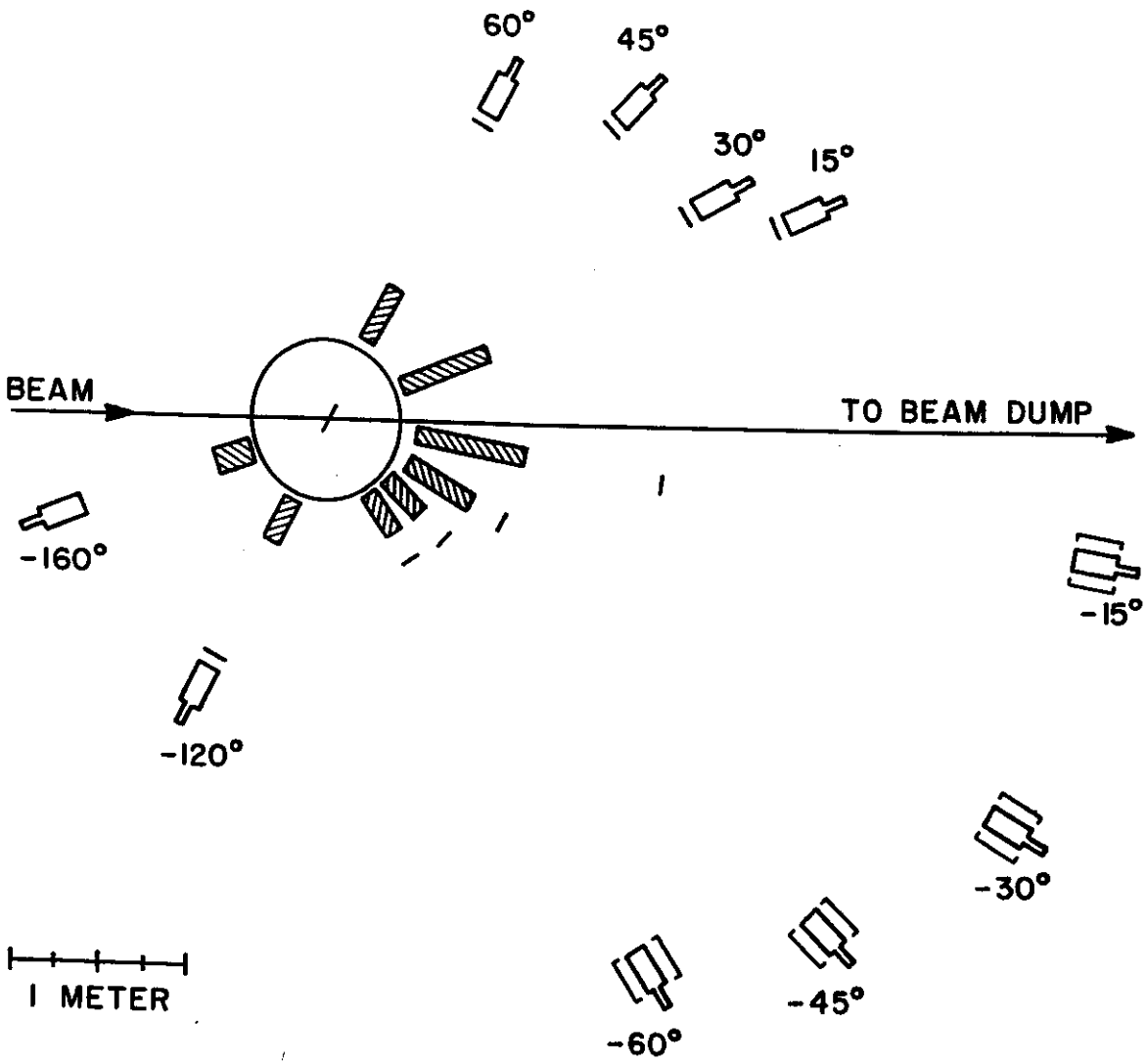

Figure 1. Experimental set-up. Groups of detectors were placed at the following angles: -15°, -30°, -45°, -60° and are enclosed in brackets. Single detectors were placed at +15°, +30°, +45°, +60°, -120° and -160°. The flight paths ranged from 160 to 450 cm. The hatched rectangular regions represent shadow bars, and the solid lines in front of detectors or shadow bars represent the proton veto paddles. The shadow bars at 30° and 45° are not shown.

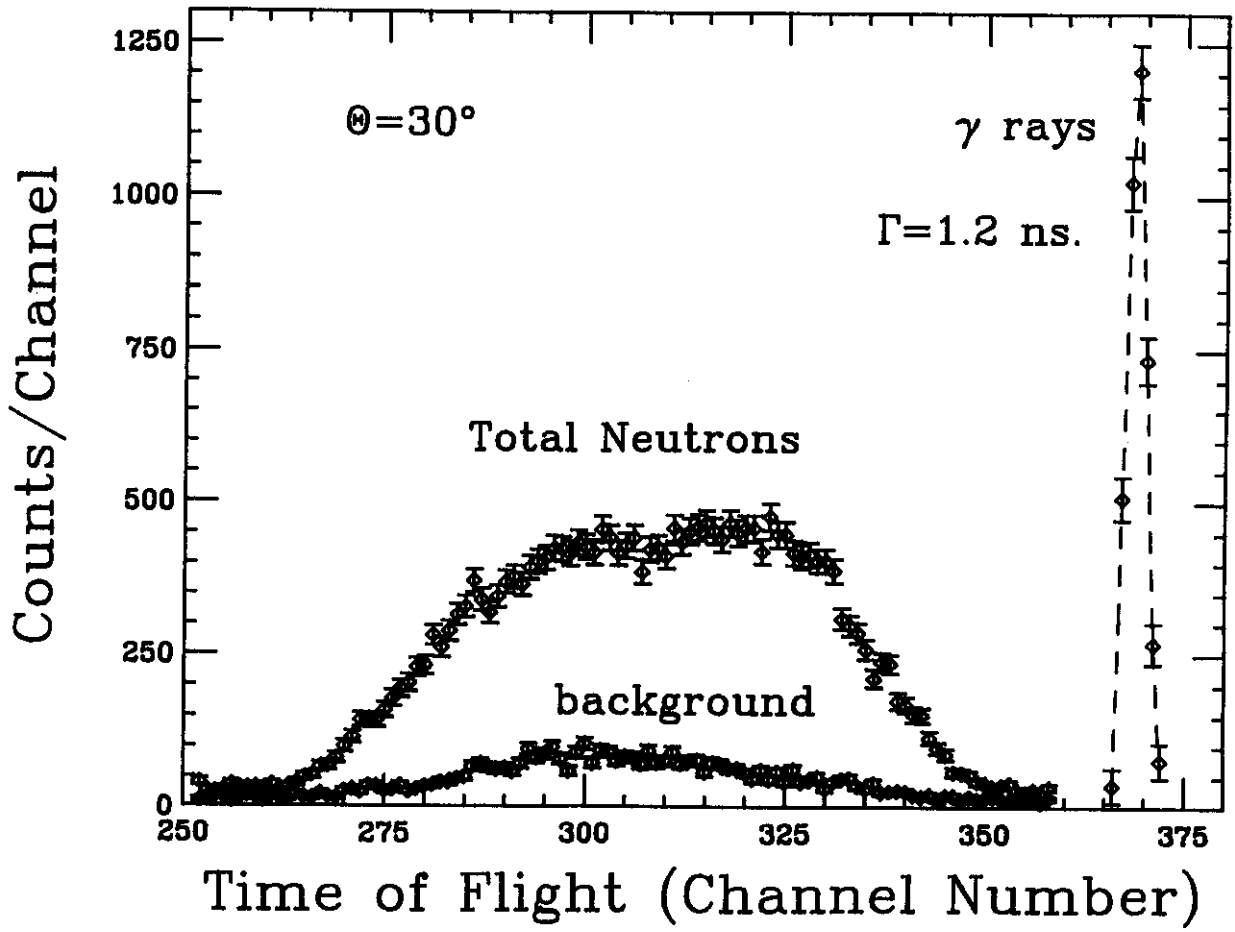

Figure 2. Typical time-of-flight spectrum for neutrons and γ rays. The data for total neutrons includes target and background contributions. The background contribution is also shown seperately. Subtracting the background from the total gives the target neutron. The width of the γ peak is 1.2 ns. The time-to-digital converter calibration is 0.2607 ns/channel.

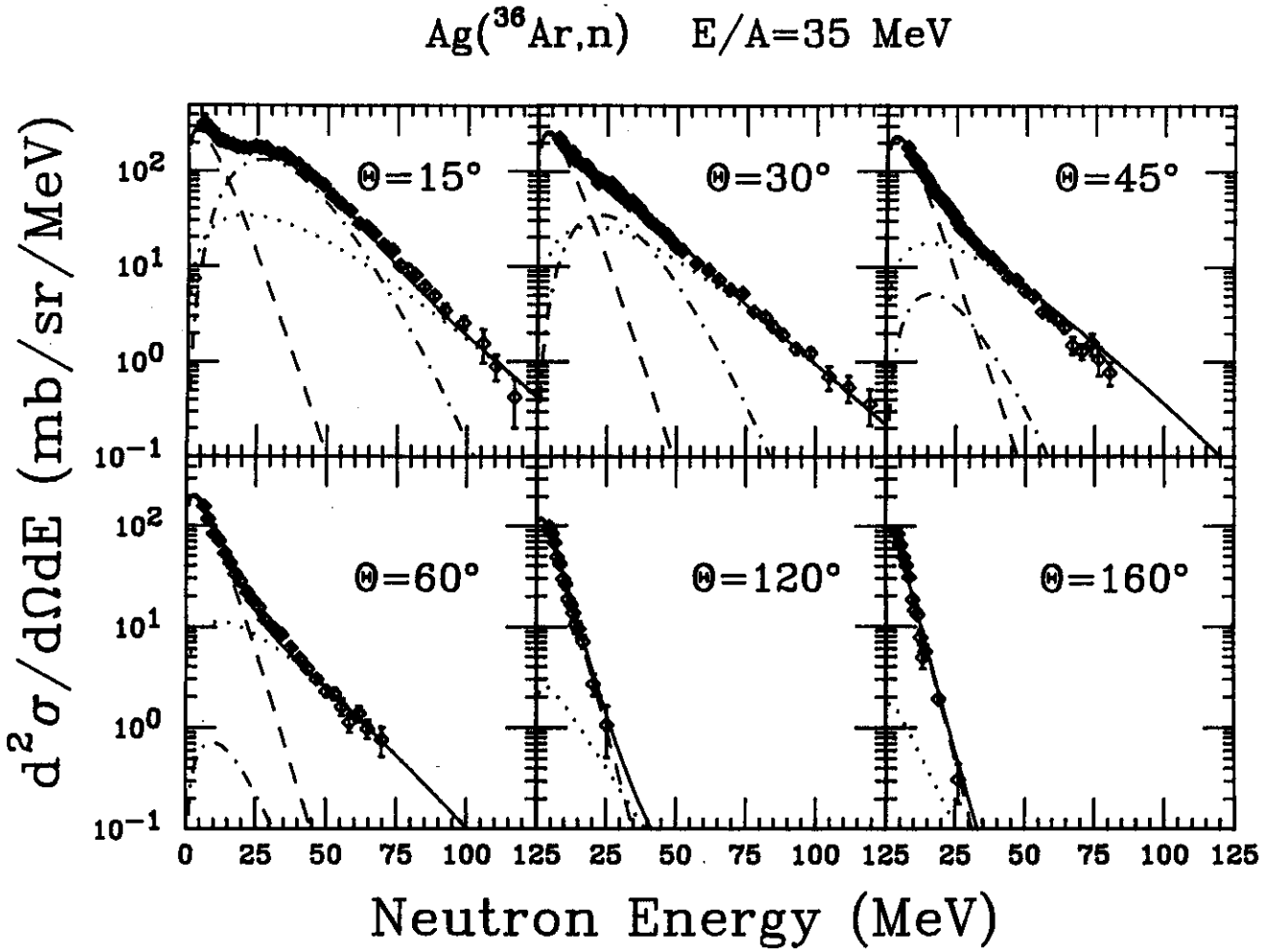

Figure 3 (a-f). The neutron energy spectra at 6 angles. The solid lines are the fits using 3 thermal sources. The dot-dashed line is the contribution from the projectile-like source, the dotted line that of the intermediate rapidity source, and the dashed line is the contribution of the target-like source.